Low-temperature specific heat of $BaCuO_2$ and $BaCuO_{2.14}$ in magnetic fields to 7 T

R. A. Fisher, D. A. Wright, J. P. Emerson, B. F. Woodfield,* and N. E. Phillips
MSD, Lawrence Berkeley National Laboratory and Department of Chemistry, University of California, Berkeley, California 94720

Z.-R. Wang† and D. C. Johnston
Ames Laboratory and Department of Physics and Astronomy, Iowa State University, Ames, Iowa 50011
(Received 20 July 1999)

The specific heats of samples of $BaCuO_2$ and $BaCuO_{2.14}$, on which magnetization and/or neutron-diffraction measurements had been made earlier, were measured for the temperature range $0.35 \leqslant T \leqslant 30$ K in magnetic fields to 7 T. $BaCuO_{2+x}$ has a complex structure with 90 formula units in a bcc unit cell; 6 Cu are ''lone spins,'' 48 are in 8 Cu_6O_{12} ''ring clusters,'' and 36 are in 2 $Cu_{18}O_{24}$ ''sphere clusters.'' The ring and sphere clusters have ferromagnetically ordered ground states with spins $S=3$ and 9, respectively. Antiferromagnetic ordering of the ring clusters occurs with a Néel temperature $T_N(0) \sim 15$ K. The specific heat of $BaCuO_2$ shows a cooperative ordering anomaly associated with the antiferromagnetic ordering of the ring clusters. Schottky-like anomalies, having maxima at ~5 and ~0.7 K, are identified with the ordering of the sphere clusters and the lone spins, respectively. Only Schottky-like anomalies are observed for the specific heat of $BaCuO_{2.14}$. It is suggested that the increase in the Cu oxidation state, due to the addition of 0.14 mol of O, increases Cu-O covalent bonding (spin compensation) and/or produces nonmagnetic Cu^{3+}, which in addition to the known increase in the Cu-O bond lengths, disrupts the superexchange paths that lead to the antiferromagnetic ordering of the ring clusters in $BaCuO_2$. For $BaCuO_2$ the magnetic entropy was 90% of that predicted for the ordering of the three Cu structures. On the other hand, the magnetic entropy for $BaCuO_{2.14}$ was only 65% of that predicted, which suggests a relative large suppression of some magnetic entities due to the addition of 0.14 mol of O. Although $BaCuO_{2+x}$ is an insulator, the specific heat has a T-proportional component that is magnetic field dependent and is presumably associated with the magnetic degrees of freedom.

I. INTRODUCTION

The deceptively simple chemical formula for nonstoichiometric $BaCuO_{2+x}$ masks the fact that it has an extremely complex crystal structure that contains 90 formula units in a body-centered-cubic (bcc) unit cell (space group $Im3m$).[1–3] There are three different systems of Cu spins within which, and between which, there are complex interactions. The Cu are all in square-planar CuO_4 units, most of which share edges to form $Cu_{18}O_{24}$ spherelike clusters and Cu_6O_{12} ringlike clusters. The bcc unit cell contains two of the spherelike clusters (36 Cu) centered on the corner and body-center positions, and eight of the ringlike clusters (48 Cu) located between the spheres and centered on the four body diagonals. There are also partially occupied sites that correspond to Cu_2O_{10} clusters, each of which can contain two CuO_4 units that *do not* share edges. In the bcc unit cell there are six of these clusters located between the spheres on the cube edges, and on parallel lines through the cube center, but the Cu sites are only 50% occupied, giving a total of six Cu of this type. These six Cu are referred to as ''lone spins.'' In $BaCuO_2$ only two of the four square-planar O sites surrounding a lone-spin Cu, the O(6) sites, are occupied on average, leaving 36 of the 48 sites of this type vacant. Both the lone-spin Cu and O are randomly distributed over the available sites in the CuO_4 units of the Cu_2O_{10} clusters. Besides the O sites in the three types of clusters, there are 12 additional occupied O sites for a total of 216 sites. As oxygen is added to $BaCuO_2$, it has been reported[1,2] that the 36 vacant O(6) sites become randomly occupied, but this assignment has been disputed[3] with the assertion that up to eight additional sites can also have variable O occupancy. The Cu sublattices in the sphere and ring clusters are independent of x.[1,2] However, as found in the cuprate superconductors, the O content influences the Cu oxidation state. The *average* valence for Cu in $BaCuO_{2+x}$ would be $2+2x$. If all 48 O(6) sites[2] were occupied, one would obtain $x=0.4$, while if only the 24 O(6) sites associated with Cu were occupied, one would have $x=0.2$, with average Cu valences of 2.8 and 2.4, respectively. However, depending on the location of the excess oxygen, the effect on the Cu oxidation state in each of the three Cu systems would not be the same. A change in oxygen content alters the Cu-O bond lengths and the unit-cell volume,[2,4] with the largest bond changes occurring in the Cu_2O_{10} clusters.[2] Changes in Cu-O bond lengths could produce related changes in the Cu oxidation state[2] and in any Cu-O-Cu superexchange paths.

Neutron-diffraction[5–7] and magnetic-susceptibility measurements[5,8] on a $BaCuO_2$ sample have shown that the lone-spin Cu has $S=1/2$, while the $S=1/2$ Cu spins in both the Cu_6O_{12} rings and $Cu_{18}O_{24}$ spheres form ferromagnetically ordered cluster ground states[7] with net spins of $S=3$ and $S=9$, respectively. (The ferromagnetic ground states are formed from the alignment of the individual $S=1/2$ Cu spins, presumably via Cu-O-Cu superexchange links.) Excited states for both types of clusters have smaller (integer) net spins. The Cu_6O_{12} ring clusters order antiferromagnetically with an ordering anomaly in magnetization at a Néel temperature $T_N(0) \sim 15$ K. Neither the lone-spin Cu nor the $Cu_{18}O_{24}$ spheres exhibit long-range magnetic order for T

$\geqslant 0.05$ K.[7] Above ~190 K the magnetization data[5,10] can be fitted with a Curie-Weiss function that is consistent with $S = 1/2$ Cu^{2+} for *all* of the Cu in $BaCuO_2$. Neutron-diffraction measurements have also been made on a $BaCuO_{2.14}$ sample.[9] At 4.2 K no cooperative, long-range magnetic order for any of the three Cu systems was observed.[9]

$BaCuO_2$ is a common impurity phase in the most widely studied of the high-T_c superconductors, $YBa_2Cu_3O_{7-\delta}$ (YBCO). The triangular phase diagram of the Y-Ba-Cu-O system allows the formation of many compounds that can occur as impurity phases in YBCO, with the more common being $Y_2Cu_2O_5$ (blue phase), Y_2BaCuO_5 (green phase), and $BaCuO_{2+x}$ (brown phase). $BaCuO_{2+x}$ has a very large specific heat at low temperatures, and it is the most troublesome of these materials with respect to its contribution to the specific heat of YBCO samples. Probably all ceramic samples of YBCO, and many ''single crystals,'' contain it as an impurity to some degree. It is stable only in a limited range of temperature and oxygen pressure, but it is metastable at ambient temperature in air.[10] $BaCuO_{2+x}$ decomposes slowly into $Ba_2Cu_3O_5$ and BaO at elevated temperatures outside the stability zone.[10]

Following the discovery of YBCO, the low-temperature specific heat (C) of $BaCuO_{2+x}$ was measured in zero magnetic field[10,12–18] and in magnetic fields (H).[10,16,17] Kuentzler *et al.*[14] were probably the first to show that the low-temperature specific heat of $BaCuO_{2+x}$ was very strongly dependent on the oxygen content, and later specific-heat measurements by others confirmed their observations.[10,15,18] All of those measurements showed that the specific heat of $BaCuO_{2+x}$ was much larger than that of YBCO at low temperatures. These findings were the source of the then widely held belief that most—if not all—of the anomalous, and highly sample dependent, $\gamma^*(0)T$ term for YBCO for $H = 0$ was probably due to the presence of varying amounts of $BaCuO_{2+x}$. Many previous samples of $BaCuO_{2+x}$ synthesized for specific-heat measurements probably contained other phases. Samples of $BaCuO_{2+x}$ have been reported[11] with x ranging from -0.21 to $+0.5$.

In this paper we report low-temperature, specific-heat measurements in magnetic fields on the two well-characterized samples of $BaCuO_{2+x}$ ($x \sim 0$ and ~0.14) used in the magnetic-susceptibility[5,8] and neutron-diffraction[5–7,9] experiments. These measurements had a fourfold purpose: (1) To measure the contributions to $C(H)$ associated with the known cooperative ordering of the Cu_6O_{12} rings and with any ordering of the $Cu_{18}O_{24}$ spheres and lone-spin Cu that might occur above ~0.35 K. (2) To observe the effect on the magnetic ordering of excess oxygen. (3) To test a model for the ordering of the three magnetic systems by evaluating the magnetic entropy. (4) To provide measurements of $C(H)$ for use in correcting specific-heat data for YBCO samples for the presence of small amounts of $BaCuO_{2+x}$.[19,20]

The sample preparation and characterization are described in Sec. II. The specific-heat measurements are described and an overview of the results presented in Sec. III. The analysis of the data to separate the lattice and magnetic contributions is described in Sec. IV, and the calculation of the magnetic entropies is described in Sec. V. Section VI includes a discussion of how changes in oxygen content affect the specific heat and entropy of $BaCuO_{2+x}$, a possible role that oxygen plays in producing the enormous changes observed in the specific heat for relatively small changes in x, and, finally, comparisons of the present data with other extensive, previously reported specific-heat measurements.[10] A general summary is given in Sec. VII.

II. SAMPLE PREPARATION

Ceramic samples,[6,8,21] ~8.5 g ($x \sim 0$) and ~9.5 g ($x \sim 0.14$), sintered as right circular cylinders, were prepared in the same way except the final heat treatment. For the $BaCuO_2$ sample the final annealing and cooling to ambient temperature were in an atmosphere of He, while one atmosphere of O_2 was used for the $BaCuO_{2.14}$ sample. No decomposition should have occurred since neither sample was held for extended periods at high temperatures outside the stability zone.[10] Based on the phase diagram in Ref. 10, the oxygen contents for the He- and O_2-annealed samples were taken to be given by $x \sim 0$ and ~0.14, respectively.

Thermogravimetric analysis (TGA) on representative samples prepared in the same ways as the two specific-heat samples gave, for a He-annealed sample, $x = 0.1 \pm 0.1$, and, for an O_2-annealed sample, $x = 0.6 \pm 0.1$.[8,21] In a recent paper[10] the upper limit on x for $BaCuO_{2+x}$ was stated to be ~0.16 for oxygen present as lattice structural elements. This value is close to the $x = 0.2$ that would be expected if the O(6) sites next to occupied Cu sites in the Cu_2O_{10} clusters were all filled. This conclusion was based on the known increase in the $BaCuO_{2+x}$ cell volume[4] with increasing oxygen content. The TGA measurement of a *surplus* $x \sim 0.46 \pm 0.1$, over the $x \sim 0.14$ expected for the O_2-annealed sample based on the phase diagram[10] (and for other samples for which even larger values of x have been reported), could be explained by the presence of strongly chemisorbed atomic oxygen (O) on surfaces or as molecular oxygen (O_2) trapped as occlusions in microscopic voids, pores, and grain boundaries of the sample, or in interstitial positions. The presence of occluded O_2 should give a thermal signature in the specific heat near 24 K due to the first-order transition of solid O_2 from the α to the β crystallographic form.[22] Specific-heat measurements on $LaCuO_{4+x}$ ($x \sim 0.13$) do have an irreversible anomaly near 24 K (Ref. 23) that is consistent with the presence of ~0.065 mol of occluded O_2. If occluded molecular oxygen is present in the $BaCuO_{2+x}$ sample and if it behaves in a similar way to that in $LaCuO_{4+x}$, then one would expect to find an anomaly in C near 24 K. Based on the results for $LaCuO_{4+x}$,[23] this anomaly would be a significant fraction of C for $BaCuO_{2+x}$. Although the specific-heat data for $BaCuO_{2+x}$ near 24 K are not closely spaced, they are very precise, and no such anomaly was observed. Therefore, it would appear that the excess of $\sim 0.46 \pm 0.1$ mol O found in the TGA analysis could be present only as strongly bound, chemisorbed O on the ceramic sample surfaces. In this paper we will assume the two samples to be $BaCuO_2$ and $BaCuO_{2.14}$ based on the conditions of preparation and the phase diagram of Ref. 10.

III. SPECIFIC-HEAT MEASUREMENTS

One end of a cylindrical sample was glued to a copper plate with GE7031 varnish and the sample covered with a

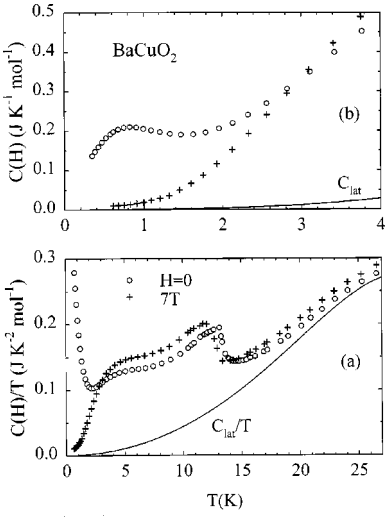

FIG. 1. The specific heat of $BaCuO_2$. (a) $C(H)/T$ vs T for $0.35<T<30$ K and $H=0$ and 7 T. For $H=0$, the antiferromagnetic and two paramagnetic ordering anomalies are clearly shown. In 7 T, the antiferromagnetic ordering anomaly has moved to a lower temperature, while the other two anomalies have both moved to higher temperatures and have coalesced into a single, broad anomaly centered at ~4.5 K. (b) $C(H)$ vs T for $T\leqslant 4$ K and $H=0$ and 7 T. The $H=0$ ordering anomaly for the lone-spin Cu in the partially occupied Cu_2O_{10} clusters is shown on an expanded scale.

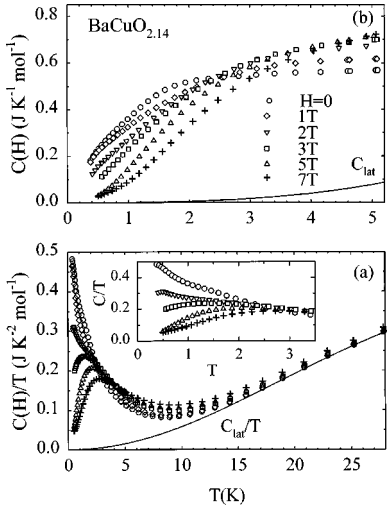

FIG. 2. The specific heat of $BaCuO_{2.14}$. (a) $C(H)/T$ vs T for $0.35<T<30$ K and $0\leqslant H\leqslant 7$ T. The inset shows the same data on an expanded scale below 3.5 K. The complex, multiple-anomaly ordering observed for $BaCuO_2$ has been replaced by single Schottky-like anomalies. (b) $C(H)$ vs T for $T\leqslant 5$ K. The Schottky-like nature of the ordering is illustrated by the H dependence.

thin layer of silver foil (also using GE7031 varnish) to ensure good thermal contact. The copper plate was screwed to the calorimeter stalk, which contained germanium and platinum resistance thermometers and a heater. The thermometers were outside the solenoid and were shielded from the magnetic field by a superconducting Nb-Ti cylinder. Specific-heat measurements were made using a semiadiabatic, heat-pulse technique[24] for $0.3\leqslant T\leqslant 300$ K and $0\leqslant H\leqslant 7$ T. The precision of the measurements was ~0.1%, while the accuracy was ~0.5%, as estimated from measurements made on a copper standard. The molecular weight of $BaCuO_2$,232.87 g mol^{-1}, was used in calculating a ''molar'' specific heat for both samples to obtain values that refer to 1 mol of Cu in both cases.

The specific heat of $BaCuO_2$ for $H=0$ and 7 T is plotted in Fig. 1(a) as C/T vs T for the entire range of temperatures of the measurements, and as C vs T in Fig. 1(b) for $T\leqslant 4$ K. The solid curves represent the lattice specific heat ($C_{\rm lat}$), which was evaluated as described below in Sec. IV. Three features are apparent in the C/T vs T plot for $H=0$. One of these features, associated with the antiferromagnetic ordering known from other measurements, appears as a relatively sharp anomaly with a peak near $T_N(0)\sim 13$ K. This peak is shifted to lower temperature in 7 T, as expected for antiferromagnetic ordering. For $H=0$, besides the antiferromagnetic ordering anomaly, there is a second broader anomaly centered at ~5 K and a sharp upturn beginning near 2 K. In 7 T, these latter two features have coalesced into a single broadened anomaly centered at ~4.5 K. In the C vs T representation in Fig. 1(b) the sharp, low-temperature upturn in C/T appears as a Schottky-like anomaly centered at ~0.7 K.

The specific heat of $BaCuO_{2.14}$ for $H=0$, 1, 2, 3, 5, and 7 T, is displayed as C/T vs T in Fig. 2(a) for the full range of temperature and in Fig. 2(b) as C vs T for $T\leqslant 5$ K. (For $H=2$ T the specific-heat data were measured only to 5 K.) The inset to Fig. 2(a) is an expanded plot of C/T vs T in the region below 3.5 K, with the curve for $H=1$ T omitted for clarity. In Figs. 2(a) and 2(b) the solid curves represent $C_{\rm lat}$. Addition of ~0.14 mol of oxygen has produced a profound change in C from that observed for the $BaCuO_2$ sample shown in Fig. 1. The antiferromagnetic ordering anomaly has disappeared, as have the other two features, and have been replaced by the broad, Schottky-like anomalies shown in the inset to Fig. 2(a) and in Fig. 2(b).

IV. DATA ANALYSIS

The lattice ($C_{\rm lat}$) and magnetic [$C_{\rm mag}(H)$] contributions to $C(H)$ were separated by an analysis of the data in the temperature region above the maxima of the ordering anomalies in C. $C_{\rm lat}$ was represented by three terms, B_nT^n ($n=3,5,7$), in the usual harmonic-lattice expansion. Although $BaCuO_2$ and $BaCuO_{2.14}$ are both insulators, and there can be no T-proportional term in $C(H)$ associated with conduction electrons, a $\gamma^*(H)T$ term was included in the fitting expression. Its inclusion substantially improved the fits for $H\neq 0$ and gave results that were consistent with an H-independent $C_{\rm lat}$. It is assumed that this term is magnetic in origin and is part of $C_{\rm mag}(H)$, i.e.,

$$C_{\rm mag}(H)=C_{\rm anmly}(H)+\gamma^*(H)T, \tag{1}$$

where $C_{\rm anmly}(H)$ is the contribution of the ''anomalies'' that are evident in Figs. 1 and 2. For $BaCuO_2$ ($H=0,7$ T) and $BaCuO_{2.14}$ ($H=0,1,3,5,7$ T), $C_{\rm lat}$ was obtained from global, least-squares fits of $C(H)$ for $15\leqslant T\leqslant 30$ K and $0\leqslant H\leqslant 7$ T to the expression

$$C_{\rm fit}(H)=A(H)/T^2+\gamma^*(H)T+B_3T^3+B_5T^5+B_7T^7, \tag{2}$$

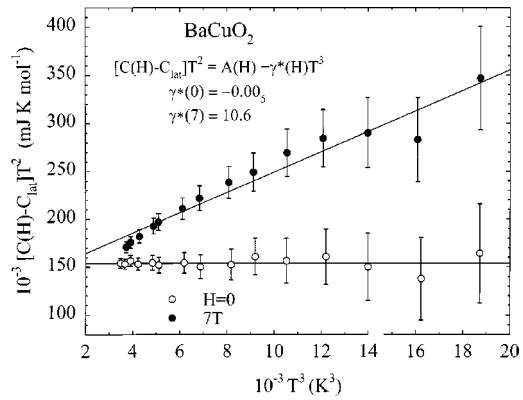

FIG. 3. $[C(H)-C_{\rm lat}]T^2$ vs T^3 for $BaCuO_2$, well above T_N, showing the high-temperature $A(H)/T^2$ magnetic terms and the $\gamma^*(H)T$ terms, which are, respectively, the intercepts and slopes of the straight lines. $\gamma^*(0)=0$. The error bars are $\pm$ 1% of $C(H)$.

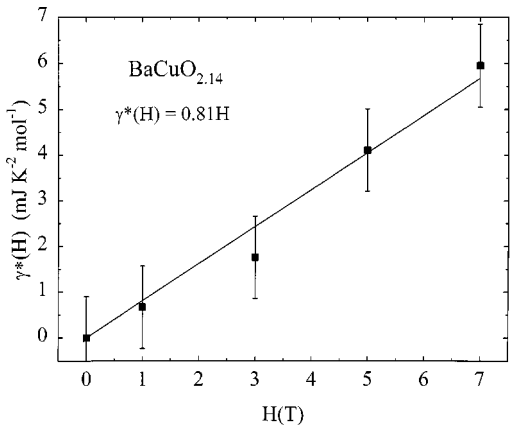

FIG. 4. $\gamma^*(H)$ vs H for $BaCuO_{2.14}$, obtained from a global least-squares fit of the data from 15 to 30 K that gave the lattice, magnetic, and $\gamma^*(H)$ parameters. The straight line represents a linear least-squares fit of $\gamma^*(H)$ to H, constrained to have zero intercept, where the error bars are $\pm$ the standard errors obtained from the global least-squares fit.

where the $A(H)/T^2$ term is used to represent the field-dependent, high-temperature-limiting form of $C_{\rm anmly}(H)$. The global fits for both samples had rms deviations of 0.34%. Addition of a B_9T^9 term to $C_{\rm lat}$ did not significantly decrease the rms deviations.

To test the reality of the $\gamma^*(H)T$ term in the $BaCuO_2$ specific-heat data, and to provide guidance in further analysis, individual fits had been made to the data for $H=0$ and 7 T *without* including a $\gamma^*(H)T$ term in the fitting expression. For $H=0$ the fit was excellent with an rms deviation of 0.08%, indicating that $\gamma^*(0)=0$. However, the fit for the 7-T data was much worse with an rms deviation of 0.50%, more than 6 times greater than for $H=0$. Moreover, the B_n coefficients were very different from those for the $H=0$ fit. $C_{\rm lat}$ obtained for the $H=0$ fit was subtracted from both the $H=0$ and 7 T data and the residuals plotted as $C_{\rm mag}T^2=[C(H)-C_{\rm lat}(0)]T^2$ vs T^3 as shown in Fig. 3. The straight line, obtained from a least-squares fit of the 7-T data, clearly establishes $\gamma^*(7T)=10.6\,{\rm mJ\,K^{-2}\,mol^{-1}}$; the plot for $H=0$ attests to the quality of the fit with $\gamma^*(0)=0$. The global fit to both sets of data gave essentially the same $C_{\rm lat}$ as that obtained in the fit to the $H=0$ data alone. A similar procedure was used to establish the presence of $\gamma^*(H)T$ terms for $BaCuO_{2.14}$. Figure 4 is a plot of $\gamma^*(H)$ vs H for the $BaCuO_{2.14}$ sample, which is linear to within the standard errors of the fitted values of $\gamma^*(H)$. The straight line represents a least-squares fit to the data, constrained to be zero for $H=0$, with a slope $\gamma^*(H)/H=0.81\,{\rm mJ\,K^{-2}\,T^{-1}\,mol^{-1}}$. The addition of $\sim$0.14 mol of oxygen to $BaCuO_2$ caused a decrease in $\gamma^*(7\,T)$ from 12.4 to 5.7 $\rm mJ\,K^{-2}\,mol^{-1}$. [The value of $\gamma^*(7\,T)$ for $BaCuO_2$ changed from 10.6 $\rm mJ\,K^{-2}\,mol^{-1}$ for the single-field fit to 12.4 $\rm mJ\,K^{-2}\,mol^{-1}$ for the global least-squares fit, which is not significant to within the accuracy of the data.] For *both* samples the adopted values for the $A(H)$ terms, the B_n lattice parameters, and the $\gamma^*(H)T$ terms were those derived from global, least-squares fits using Eq. (1) and constraining $\gamma^*(0)$ to be zero. These parameters are only slightly different from those obtained from the single-field fits and are believed to be more representative since all fields were used to establish them. It is not possible to derive reliable values of $\gamma^*(H)$ from fits to the low-temperature data since the magnetic ordering anomalies make significant contributions to $C(H)$ in the low-temperature region, and they cannot be uniquely modeled. However, the assumption that the $\gamma^*(H)T$ terms obtained from the analysis of the data for $T>15$ K are also present at low temperatures is consistent with the low-temperature data.

A nuclear hyperfine specific heat ($C_{\rm hf}$) is expected for the nuclei ^{63,65}Cu and ^{135,137}Ba, whose combined theoretical contributions are given in the high-temperature limit by $C_{\rm hf}(H)=0.003\,29(H/T)^2\,{\rm mJ\,K^{-1}\,mol^{-1}}$ for H in tesla. In the temperature range of the present measurements, $C_{\rm hf}(H)$ makes only a small contribution [$\sim$1% of $C(7\,{\rm T})$ at 0.6 K], and the only evidence for its presence is a very small upturn in the lowest data point in $C(7\,{\rm T})$ and $C(7\,{\rm T})/T$ for the $BaCuO_2$ sample. This upturn is much too small to be seen in the plots shown in Fig. 1 and is only observable on an expanded scale. Despite its small contribution, the calculated $C_{\rm hf}(H)$ was subtracted from all $C(H)$ data before any entropy evaluations were made.

The global least-squares fits gave $B_3=0.425$ $\rm mJ\,K^{-4}\,mol^{-1}$ for $BaCuO_2$ and $B_3=0.620\,{\rm mJ\,K^{-4}\,mol^{-1}}$ for $BaCuO_{2.14}$. The limiting, low-temperature Debye thetas (Θ_D) are, respectively, 264 and 233 K, where $\Theta_D=[(12/5)\pi^4N_Ak_BN_{\rm atom}/B_3]^{1/3}$, N_A is the Avogadro number, k_B the Boltzmann constant, and $N_{\rm atom}$ the number of atoms in the formula unit—4 for $BaCuO_2$. Figure 5 is a plot of $C_{\rm lat}/T^3$ vs T for both samples. The solid curves show the temperature region of the global, least-squares fits used to obtain the B_n. The addition of oxygen to $BaCuO_2$ produces a softening of the lattice modes, particularly the low-frequency acoustic modes that determine B_3.

Figure 6(a) is a plot of the magnetic specific heat $C_{\rm mag}(H)/T=[C(H)-C_{\rm lat}]/T=[C_{\rm anmly}(H)+\gamma^*(H)T]/T$ vs T, and Fig. 6(b) shows $C_{\rm mag}(H)=[C(H)-C_{\rm lat}]$ vs T for $BaCuO_2$. It is obvious from these plots that there are relatively large amounts of short-range order—antiferromagnetic correlations—above $T_N(H)$. Similar plots are shown in Figs. 7(a) and 7(b) for $BaCuO_{2.14}$. The anomalies in $[C(H)-C_{\rm lat}]$ vs T in Fig. 7(b) are Schottky-like, and the offsets at higher temperatures clearly show the influence of the

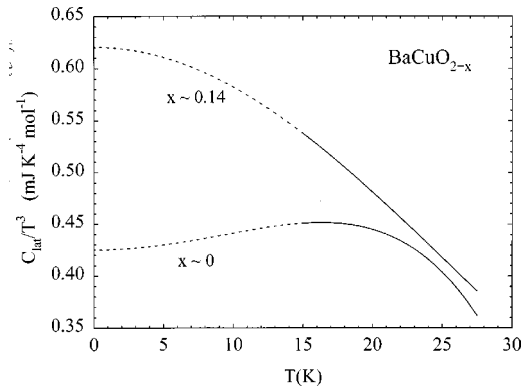

FIG. 5. $C_{\rm lat}/T^3$ vs T for $BaCuO_{2+x}$ for $x\sim 0$ and ~ 0.14. The solid curves show the temperature regions of the global least-squares fits used to obtain the B_n, while the dashed curves are extrapolations using those B_n. Evidently, increasing the oxygen content from ~ 2 to ~ 2.14 causes a softening of at least some of the lattice modes.

$\gamma^*(H)T$ component of $C(H)$. As shown in Fig. 7(b), the shift of the maxima in $[C(H)-C_{\rm lat}]$ to higher T with increasing magnetic field is much less than would have been expected for a simple Schottky function. (The ratio of the shifts in the maxima of $[C(H)-C_{\rm lat}]$ for $H=7$ T and 1 T is 1.5 compared with a corresponding shift in this ratio of ~ 7—greater than a factor of 4—for simple Schottky functions with $g=2$, $S=1/2$, 3, and 6, and no crystal-field splitting.)

Evidently, the long-range antiferromagnetic ordering for $BaCuO_2$ (seen in Fig. 6) has been destroyed by the addition of oxygen. These results are consistent with neutron-diffraction measurements,[9] which also show no cooperative, long-range order. When the curves in Fig. 6 are compared to those in Fig. 7, the contrast in the specific heat and its magnetic-field dependence, caused by the addition of only ~ 0.14 mol of oxygen, is striking. Obviously, the nature of the ordering has been dramatically altered.

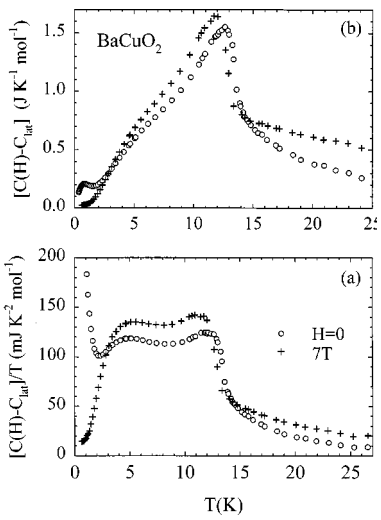

FIG. 6. The magnetic specific heat for $BaCuO_2$ obtained after subtracting $C_{\rm lat}$ from the data shown in Fig. 1. In (a) the data are plotted as $[C(H)-C_{\rm lat}]/T$ vs T for $H=0$ and 7 T; in (b) as $[C(H)-C_{\rm lat}]$ vs T.

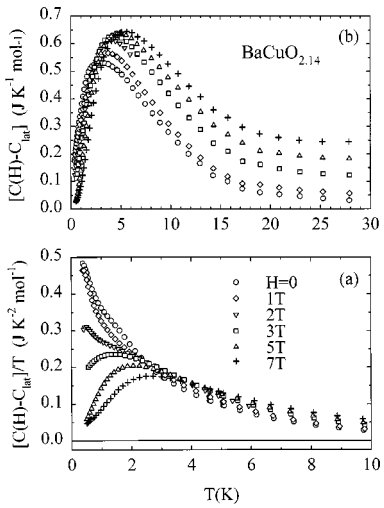

FIG. 7. (a) A plot of $[C(H)-C_{\rm lat}]/T$ vs T below 10 K for $BaCuO_{2.14}$, emphasizing the low-temperature ordering. The data for $H=0$ show a small feature between 1 and 2 K. (b) The same data as (a) but plotted as $[C(H)-C_{\rm lat}]$ vs T for $0.35<T<30$ K. This plot emphasizes the short-range Schottky-like nature of the ordering, while at high temperatures the displacements of the curves with field shows the presence of $\gamma^*(H)T$ terms. The temperature shift of the maxima in $[C(H)-C_{\rm lat}]$ with magnetic field is relatively small compared to the shift observed for a simple Schottky function. Note the sharp contrast between the specific-heat data shown in this figure for $BaCuO_{2.14}$ and that for $BaCuO_2$ shown Fig. 6.

V. MAGNETIC ENTROPY

To obtain the entropy $[S_{\rm mag}(H)]$ for the magnetically ordered entities for the two samples and their high-temperature limiting values for $H=0$ ($S_{\rm lim}$), $\int C_{\rm mag}(H)/T\,dT$—corrected for $C_{\rm hf}(H)$—was evaluated for three separate regions: From $T\sim 0.35$ to ~ 30 K, the data were integrated numerically. For $T\lesssim 0.35$ and $T\gtrsim 30$ K, they were extrapolated to $T=0$ and $T=\infty$, to obtain, respectively, $\Delta S_{\rm LT}(H)$ and $\Delta S_{\rm HT}(H)$, the contributions to $S_{\rm mag}(H)$ from those regions. To make extrapolations to the absolute zero, $C_{\rm mag}(H)$ in the lower end of the temperature range was fitted using the $\gamma^*(H)T$ terms derived at high temperature—where they were necessary for a good fit—plus the limiting, low-temperature expression for a two-level Schottky anomaly:

$$C_{\rm mag}(H)=\gamma^*(H)T+nN_Ak_B[E(H)/T]^2e^{-E(H)/T}, \quad (3)$$

where n is the number of moles and $E(H)$ is the splitting (in kelvin) between the ground and excited state. This form for the extrapolation of $C_{\rm anmly}(H)$, the second term in Eq. (3), is used as a reasonable empirical fitting expression. However, no theoretical significance should be attached to the derived parameters since the data being fitted do not correspond to a single Schottky function. This is shown, e.g., by the fact that n is not field independent, which it would be if the data corresponded to a single Schottky anomaly. [An extrapolation of $C_{\rm mag}(H)$ to $T=0$ was also made using a polynomial fit that gave the same value of $\Delta S_{\rm LT}(H)$ to better than 1%, emphasizing that the extrapolated entropy is not strongly dependent on the form of the expression used.] Values of $A(H)$ from the global, least-squares fit of C at high T to Eq. (2) in Sec. IV were used to evaluate $\Delta S_{\rm HT}(H)$ from T

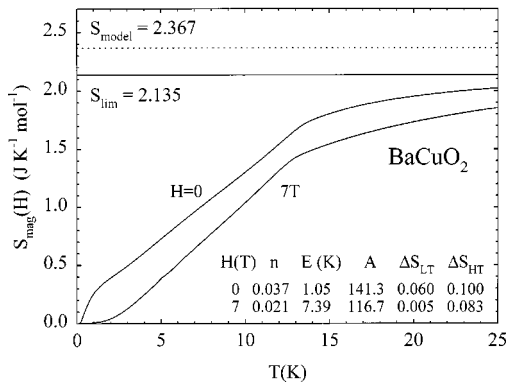

FIG. 8. The magnetic entropy derived from the specific heat for $BaCuO_2$ plotted as $S_{mag}(H)$ vs T. The $H=0$ curve extrapolates to the limiting entropy shown by the horizontal straight line. With an assumption about the $\gamma^*(H)T$ term (see text) the 7-T curve extrapolates to the same limit. This limiting entropy is 10% lower than that expected for the ordering of the three structural Cu-O units, which is shown by the horizontal dotted line. The parameters used in the low- and high-temperature extrapolations are given in the table in the figure, where the units are T, K, J, and mol.

$\sim 30\,\mathrm{K}$ to ∞: $\Delta S_{HT}(H)=A(H)/(2T_{extp}^2)$, where $T_{extp}\sim 30\,\mathrm{K}$ is the starting temperature for the extrapolation. For both samples and all H, the maximum contribution of $\Delta S_{LT}(H)$ and $\Delta S_{HT}(H)$ to S_{lim} is each $\leqslant 5\%$.

Figures 8 and 9 show $S_{mag}(H)$ as a function of T for $BaCuO_2$ and $BaCuO_{2.14}$ (the $H=1$ T data have been omitted for clarity), respectively. Included in the figures are the parameters used in the low- and high-temperature entropy extrapolations, and their values ΔS_{LT} and ΔS_{HT}, respectively. For $BaCuO_2$, $S_{lim}=2.135\,\mathrm{J\,K^{-1}\,mol^{-1}}$ and for $BaCuO_{2.14}$, $S_{lim}=1.525\,\mathrm{J\,K^{-1}\,mol^{-1}}$. The values of $S_{mag}(H)$ extrapolated to $T=\infty$ for $H\neq 0$ are significantly smaller than the values for $H=0$ for both samples.

For both $BaCuO_2$ and $BaCuO_{2.14}$ the excited states of the ring and sphere clusters are believed to be at such high

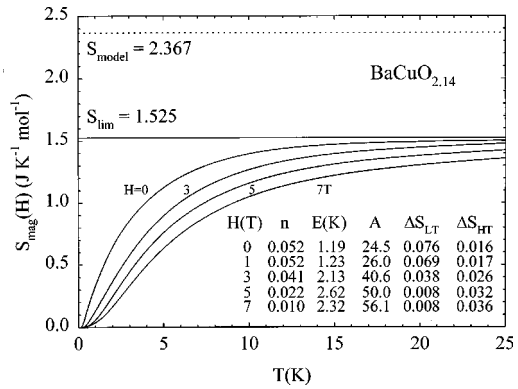

FIG. 9. A plot of $S_{mag}(H)$ vs T for $BaCuO_{2.14}$, similar to that shown in Fig. 8 for $BaCuO_2$. Inclusion of the $\gamma^*(H)T$ entropy above ~ 30 K for the $H\neq 0$ data (see text) makes all curves extrapolate to the same limiting entropy (shown as a horizontal solid line) to within 1%. This limiting entropy is 35% smaller than the value expected for ordering of the three structural Cu-O subunits, which is shown as the horizontal dotted line. The parameters used in the low- and high-temperature extrapolations are listed in the table in the figure, where the units are T, K, J, and mol.

energies[8] that specific-heat measurements below 30 K would include only contributions from the ordering of those clusters in their ground states and the ordering of the lone spins. Consequently, the values of $S_{mag}(H)$ (extrapolated to $T=\infty$) should be independent of H. However, the dependence of $S_{mag}(H)$ on H, noted above, is consistent with the interpretation that the $\gamma^*(H)T$ term in $C(H)$ is of magnetic origin, and its contribution to the entropy should be included in $S_{mag}(H)$. Obviously, there must be a ''cutoff'' to that contribution to avoid an infinity in the entropy. Since there is no apparent basis for modeling the ''cutoff,'' it was taken as a discontinuous drop to zero at a temperature T_0, which might be expected to depend on both x and H, to give

$$S_{mag}(H)=S_{anmly}(H)+\gamma^*(H)T_0. \tag{4}$$

For $BaCuO_2$, $T_0=40.4\,\mathrm{K}$ makes $S_{mag}(7\,\mathrm{T})=2.135\,\mathrm{J\,K^{-1}\,mol^{-1}}$ at $T=\infty$, the value of S_{lim}. In the case of $BaCuO_{2.14}$, $T_0=45.0\,\mathrm{K}$ gave $S_{mag}(H)=1.555$, 1.555, 1.546, and $1.521\,\mathrm{J\,K^{-1}\,mol^{-1}}$ for $H=1$, 3, 5, and 7 T, respectively, with an average of $1.544\pm 0.015\,\mathrm{J\,K^{-1}\,mol^{-1}}$, compared with $S_{lim}=1.525\,\mathrm{J\,K^{-1}\,mol^{-1}}$. [A combination of magnetization measurements and model calculations[10] has been interpreted as showing a T-proportional term in $C(H)$ for $H\neq 0$ that begins to decrease near 30 K and vanishes above 50 K.] S_{lim} for both samples is much smaller than $R\ln[2(1/2)+1]=5.764\,\mathrm{J\,K^{-1}\,mol^{-1}}$ that naively might have been anticipated for 1 mol of Cu^{2+} in $BaCuO_2$ if no microscopic structural information had been available. A reduction in the entropy is expected, however, because of the high-temperature formation of the eight Cu_6O_{12} ring clusters with ferromagnetic Cu ordering ($S=3$) plus the two $Cu_{18}O_{24}$ sphere clusters with ferromagnetic Cu ordering ($S=9$), which removes a large fraction of the $R\ln 2$ entropy for free Cu^{2+} spins with $S=1/2$. Theoretically, the entropy associated with each of the three structural units in the unit cell is, (1) $S_{1s}=(6/90)R\ln[2(1/2)+1]=0.384\,\mathrm{J\,K^{-1}\,mol^{-1}}$, (2) $S_r=(8/90)R\ln[2(3)+1]=1.438\ \mathrm{J\,K^{-1}\,mol^{-1}}$, and (3) $S_s=(2/90)R\ln[2(9)+1]=0.544\ \mathrm{J\,K^{-1}\,mol^{-1}}$, where $1s$, r, and s refer, respectively, to the lone spins, rings, and spheres. The three contributions to the magnetic entropy for the model have a sum $S_{model}=2.366\,\mathrm{J\,K^{-1}\,mol^{-1}}$. The $BaCuO_2$ and $BaCuO_{2.14}$ samples have S_{lim} that are, respectively, 10% and 35% lower than S_{model}. Furthermore, there can be no entropy ''hidden'' below $T\sim 0.35\,\mathrm{K}$ associated with an anomaly in C for $H=0$ to account for these discrepancies. If such ''hidden'' entropy existed for $H=0$, the 7-T field would have shifted the associated anomaly in $C(7\,\mathrm{T})$ to well above 0.35 K. The difference in magnetic entropy between $BaCuO_2$ and $BaCuO_{2.14}$ reinforced the conclusion, reached from an examination of $C_{mag}(H)$ in Figs. 6 and 7 of Sec. IV, that the addition of excess oxygen produces a fundamental change in the magnetic ordering.

VI. DISCUSSION

A. Specific heat and entropy of $BaCuO_2$

Figure 6 shows specific-heat anomalies in three distinct regions of temperature, near 0.7, 5, and 13 K. From the magnetization and neutron-diffraction data,[5–8] one expects these anomalies to be associated with the ordering of the lone

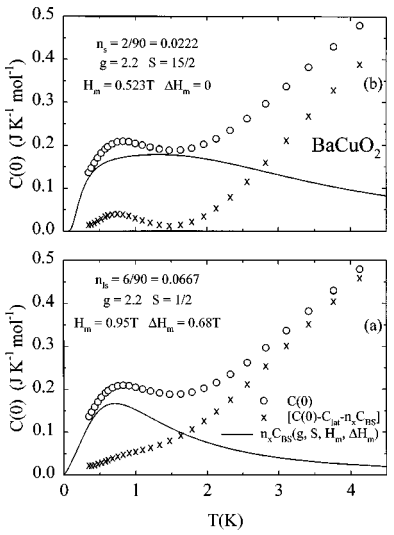

FIG. 10. (a) The low-temperature anomaly for $BaCuO_2$, which is identified with the ordering of the lone-spin Cu in the partially occupied Cu_2O_{10} clusters, is shown as open circles. The solid curve is a Gaussian-broadened, Schottky function (C_{BS}) with parameters selected (and shown in the figure) to give the ''best'' fit to the anomaly and to have the correct entropy. The ''best'' C_{BS} was taken to be the one that minimized the structure remaining in $[C(0)-C_{lat}-C_{BS}]$ as shown by the *x* symbols. A small amount of structure remains, but overall the fit is good. (b) The same as (a) except the fit is for two ferrimagnetic clusters, each with spin 15/2, formed from the antiferromagnetic coupling of a sphere cluster with three lone-spin partially occupied Cu_2O_{10} clusters. The ''best'' calculated curve for the fit to the ferrimagnetic clusters is too broad to fit the data.

spins $[n_{ls}=6/90\ \text{mol (mol BaCuO}_2)^{-1},\ S=1/2]$, the $Cu_{18}O_{24}$ spheres $[n_s=2/90\ \text{mol (mol BaCuO}_2)^{-1},\ S=9]$, and the Cu_6O_{12} rings $[n_r=6/90\ \text{mol (mol BaCuO}_2)^{-1},\ S=3]$. The 13-K anomaly is obviously associated with the long-range antiferromagnetic ordering of the rings, which is known to occur at that temperature.[5–8] It also has the shape and magnetic field dependence expected for an exchange-driven, cooperative, antiferromagnetic transition. The 0.7- and 5-K anomalies are, therefore, to be associated with the ordering of the lone spins and the spheres. Both anomalies have a Schottky-like appearance that suggests crystal-field and/or molecular-field interactions. The 0.7-K anomaly is relatively amenable to analysis, and it will be shown below to be more consistent with ordering of the lone spins, leaving the 5-K anomaly for the ordering of the sphere spins.

Figure 10(a) shows the 0.7-K anomaly compared with a Gaussian-broadened Schottky function (C_{BS}) for $n_{ls}=6/90\ \text{mol (mol BaCuO}_2)^{-1}$ represented by the solid curve. (Broadening could be produced by the known inhomogeneous oxygen distribution[2,3,9] in $BaCuO_2$.) Fit parameters are given in the figure where S is the spin, g the spectroscopic splitting factor, H_m the molecular field, and ΔH_m the Gaussian broadening parameter for the magnetic field. (For Cu^{2+}, $g\sim2.2$ is quite common, but the particular choice is not crucial to the fit since the Gaussian-broadened Schottky parameters are the products gH_m and $g\Delta H_m$. Choosing different values for g produces compensating changes in both H_m and ΔH_m). By fixing $n_{ls}=6/90\ \text{mol (mol BaCuO}_2)^{-1}$ and $S=1/2$, the associated entropy is the expected 0.384 $\text{J K}^{-1}\text{mol}^{-1}$ for the ordering of the Cu in the partially occupied Cu_2O_{10} clusters. The $\times$ symbols in Fig. 10(a) represent the specific heat remaining after subtracting both C_{lat} and $n_{ls}C_{BS}$ from C. After the subtractions, there is still a small feature in C below $\sim$1 K. Nonetheless, representation of the lowest anomaly by the Gaussian-broadened Schottky function is quite good.

Based on the behavior of the low-temperature magnetization data for $T\geqslant2$ K, it was proposed[5] that the three Cu spins in three partially occupied Cu_2O_{10} units were antiferromagnetically coupled to a sphere cluster to form ferrimagnetic clusters with net spin $S=15/2$ at low temperature. Two such clusters would be formed per unit cell with a concentration $n_s=2/90\ \text{mol (mol BaCuO}_2)^{-1}$. The exchange constant[5] derived from a fit of the magnetization data to this ferrimagnetic complex model had an energy scale of $\sim$4.5 K. It was also suggested that these ferrimagnetic clusters might order near 1 K.[5] For this model, it would follow that the anomaly in C near 5 K would be identified with the formation of the ferrimagnetic clusters and the anomaly in C at $\sim$0.7 K with their ordering in a molecular magnetic field. However, it is not possible to achieve a good fit of the specific-heat data to a Schottky function assuming such ferrimagnetic clusters. If the $S=15/2$ manifold of the complex is assumed to be split into 16 equally spaced energy levels in a molecular-magnetic field, which is the only fit variable, any calculated anomaly that falls in the temperature interval required by the data is too broad as illustrated in Fig. 10(b). Based on the results of the two fits, the 0.7-K anomaly is not consistent with ordering of the proposed ferrimagnetic clusters, and there is no calorimetric evidence for their existence. This conclusion is not inconsistent with the magnetization data[5] since the field and temperature dependence of those data can also be explained if the sphere clusters are ordering due to crystal–electric-field and/or molecular–magnetic-field splitting of the energy-level manifold. The same argument that the 0.7-K anomaly could not be associated with ordering of the ferrimagnetic clusters applies to the sphere clusters. Consequently, it is, for several reasons, the 5-K anomaly that is to be associated with the short-range ordering of the sphere clusters.

Dipole-dipole interactions are far too weak to account for the ordering of the lone spins at 0.7 K, and for the sphere clusters at 5 K. Crystal-field interactions may play a role for the sphere clusters, but not for the lone spins for which $S=1/2$. Molecular-magnetic fields arising from other ordered spin systems—from the rings for the spheres, and from both the rings and spheres for the lone spins—are probably important in both cases. Several examples of experimental evidence of such interactions have been reported,[25–28] and in a particular case two theoretical interpretations were proposed.[29,30]

The derived magnetic entropy for $BaCuO_2$ is 2.135 $\text{J K}^{-1}\text{mol}^{-1}$, which is 10% lower than that expected for the model of six lone spins, eight ring clusters in their ground states ($S=3$), and two sphere clusters in their ground states ($S=9$). Two explanations could account for this discrepancy: (1) If some crystal-field levels for either, or both, the ring and sphere clusters were shifted to energies well above 30 K, they would make only a negligible contribution to the specific heat and entropy deduced from $C(H)$. For example,

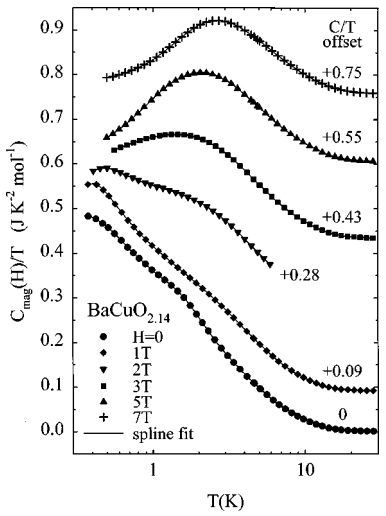

FIG. 11. $C_{\mathrm{mag}}(H)/T$ vs $\log T$ for $BaCuO_{2.14}$ with the points offset by an increasing additive amount for each field. This plot shows the small features in the low-field specific heats and the Schottky-like anomalies in the higher fields. The curves through the data points are spline fits, which serve as guides to the eye.

such a displacement for two of the seven levels for the ring clusters could account for the missing entropy. Such a displacement of two of the energy levels might also explain the ordered magnetic moment of ~ 0.89 Bohr magnetons per Cu in the ring clusters, computed from the neutron-diffraction measurements,[5,7] which is smaller than $gS\mu_B \sim (2.2)(1/2)\mu_B \sim 1.1\mu_B$ per Cu anticipated. (2) The value of $x \sim 0$ is only nominal, and small amounts of excess oxygen might be present. Furthermore, even if $x=0$, an inhomogeneous distribution of the oxygen could still exist.[2,3,9] In either case, an increase in the Cu oxidation state to greater than $+2$, due to the presence of an excess or an inhomogeneous distribution of oxygen, could cause some spins to be suppressed either through covalent bonding (spin compensation) or the production of nonmagnetic Cu^{3+}—see Sec. VI B for additional details. This would result in a reduction in entropy. Neither possibility can be ruled out by any of the existing measurements.

B. The specific-heat and entropy of $BaCuO_{2.14}$

The addition of ~ 0.14 mol O per mol $BaCuO_2$ suppresses the cooperative antiferromagnetic ordering of the Cu_6O_{12} ring structures. The specific-heat results are supported by the neutron-diffraction measurements,[9] which show no cooperative long-range order. Figure 7(b) shows that $C_{\mathrm{mag}}(H)$ vs T has Schottky-like anomalies for all fields. These anomalies have replaced the two Schottky-like anomalies and the long-range antiferromagnetic ordering anomaly shown in the very structured plot of $C_{\mathrm{mag}}(H)$ vs T in Fig. 6. However, for $H=0$, 1, and 2 T the Schottky-like anomalies in Fig. 7(b) are not ''ripple free.'' This is shown more clearly in Fig. 11, which is a plot of $C_{\mathrm{mag}}(H)/T$ vs $\log T$ with the data for different H offset by different amounts for clarity. (The curves through the data are spline fits that serve as guides to the eye.) For $H=0$, 1, and 2 T there are two features whose separations, magnitudes, and temperature placements vary with H. In magnetic fields of 3, 5, and 7 T there are only single, fully developed, Schottky-like anomalies.

The addition of ~ 0.14 mol O would produce an *average* Cu valence of 2.28 in $BaCuO_{2.14}$. Although the effects on individual Cu will depend on the sites occupied by the oxygen and homogeneity of its distribution,[2,3,9] there is a general increase in the oxidation state of the Cu. This increase in the oxidation state of Cu could promote covalent Cu-O bonding (spin compensation) and a subsequent loss of antiferromagnetic ordering. Formation of Cu^{3+}, which is also a possibility, would result in a singlet ground state and a loss of magnetization. This could also suppress cooperative long-range ordering.

The specific-heat and entropy can be understood by adopting a scenario that the addition of the excess oxygen produces changes in both the Cu oxidation state and Cu-O bond lengths, which could cause suppression of magnetic states through covalent bonding, as in the cuprate superconductors. Oxygen will, presumably, randomly occupy the various available sites,[2,3,9] and magnetism could be quenched for some members in all three systems. A random quenching of the magnetism in some ferromagnetic Cu_6O_{12} ring clusters could disrupt the exchange interaction between them, with the subsequent destruction of antiferromagnetic order. With the addition of sufficient oxygen, three different, interacting paramagnetic systems would remain. Two of these systems would be the ring and sphere clusters, with their ground states perhaps split by crystal-electric fields. The third system would be Cu with $S=1/2$ in the lone-spin partially occupied Cu_2O_{10} clusters. Ground-state doublets for these Cu would be split by a combination of dipole-dipole interactions and possible molecular magnetic fields produced by short-range (spin-glass-like) ordering of the ring and/or sphere clusters. The measured specific heat would consist of a superposition of specific heats for these three interacting paramagnetic systems. Since the number of energy levels and their splitting would be different for each system, structure in $C(H)$ probably would be observed for $H=0$ and in low magnetic fields, as shown in Fig. 11. The separations between the energy levels for each of the three systems change as H increases. This magnetic-field-induced change in the energy levels will produce an overlap of the specific-heat contributions of the three systems. This overlap would result in a smoothing of $C(H)/T$ vs T, as shown in Fig. 11 for $H=3$, 5, and 7 T.

For a heuristic interpretation of the Schottky-like character of the $C_{\mathrm{anmly}}(H)$, the data were fitted to a single Schottky function $nC_{\mathrm{Sch}}(\langle S\rangle, g\langle H_m\rangle)$, with no Gaussian broadening, where n represents the total number of moles of *all* magnetically active units for the three different systems, $\langle S\rangle$ is an average spin value for the three systems, g the spectroscopic splitting factor, and $\langle H_m\rangle$ an average molecular-magnetic field. The product gH_m always occurs as a combination variable in the C_{Sch} expression, and allows for the presence of both molecular-magnetic fields and any variations of g with field. In all of the calculations described below, g was fixed at 2.

The fitting was done in three stages: (1) The $C_{\mathrm{anmly}}(H)$ data for each field were fitted separately with n, $\langle S\rangle$, and $\langle H_m\rangle$ as variables. (2) In a second fit, $\langle S\rangle$ derived from the first fit, which was neither an integer nor a half-integer, was rounded to the nearest integer/half-integer and held fixed with only n and $\langle H_m\rangle$ as variables. There was only a negli-

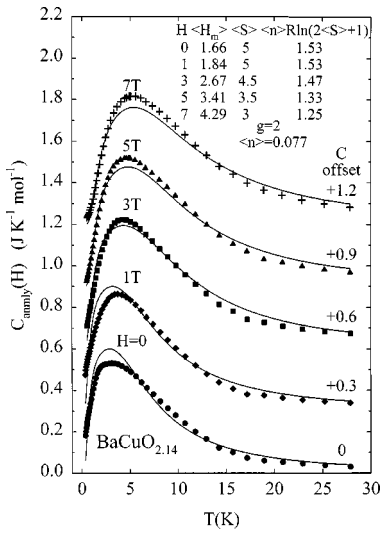

FIG. 12. A plot of $C_{\mathrm{anmly}}(H)$ vs T for $H=0$, 1, 3, 5, and 7 T for $BaCuO_{2.14}$, with the data for each field offset by an increasing additive amount. The curves represent least-squares fits to the data using unbroadened Schottky functions, a constant number of moles of magnetic units, $\langle n\rangle$, and no splitting of the energy levels other than that produced by $\langle H_m\rangle$. The fit parameters ($\langle S\rangle$ and $\langle H_m\rangle$) are functions of the applied magnetic field and are tabulated in the figure.

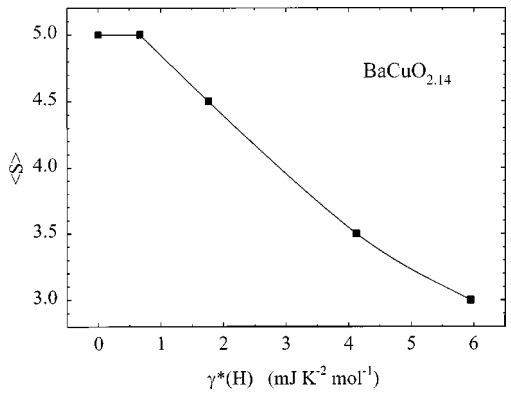

FIG. 13. The average values of spin, $\langle S\rangle$, obtained from the fits shown in Fig. 12, are plotted versus $\gamma^*(H)$. The decrease in $\langle S\rangle$ with H is accompanied by an increase in $\gamma^*(H)$. The spline curve through the points serves as a guide to the eye.

gible change in the quality of the fit. The variables n and $\langle S\rangle$ both decrease in going from $H=0$ to 7 T, with n ranging from 0.085 to 0.065 (a factor of 0.77) and $\langle S\rangle$ changing from 15/2 to 5/2 (a factor of 3). $\langle S\rangle$ and n are not completely independent variables since the amplitude of the Schottky anomaly depends on both. (3) For the final, single-field fits, an average value of n was used, $\langle n\rangle=0.077$ mol of magnetic units, where $\langle n\rangle$ is the sum of an unknown combination of magnetically active rings, spheres, and lone-spin Cu. In these fits only $\langle S\rangle$ and $\langle H_m\rangle$ were variables, with the constraint that $\langle S\rangle$ is either an integer or half-integer. Figure 12 is a plot of offset $C_{\mathrm{anmly}}(H)$ vs T for $H=0$, 1, 3, 5, and 7 T with a tabulation of the fit parameters included in the figure. The solid curves in Fig. 12 represent the fitted Schottky curves. The agreement between the data and the simplistic Schottky fit is a surprisingly good one considering that both $\langle S\rangle$ and $\langle H_m\rangle$ are averages for the three different magnetic systems in $BaCuO_{2.14}$. These simple Schottky functions agree reasonably well with $C_{\mathrm{anmly}}(H)$ over the entire temperature range, $0.35<T<30$ K, with the agreement being better for $H=3$, 5, and 7 T. A Gaussian-broadened Schottky function would improve the quality of the fit for $H=0$ and 1 T. The effect of an applied magnetic field on the temperature of the maxima in the curves is surprisingly small and is reflected in the small increase of $\langle H_m\rangle$ with increasing H.

Of the 90 Cu in a unit cell of $BaCuO_{2+x}$, there are six lone-spin Cu, eight ring clusters, and two sphere clusters, or $16/90=0.178$ mol of magnetic units compared to $\langle n\rangle=0.077$ mol. The value of 0.178 mol of magnetic units was approximately correct for $BaCuO_2$—see Sec. IV. Evidently, the assumed random addition[2,3,9] of ~0.14 mol of oxygen to various sites in $BaCuO_2$ suppressed S for a large fraction of the spins—more than 50%—in the various Cu systems. Presumably, those changes in S resulted from an increase of the oxidation state for some Cu to values exceeding +2. The *decrease* in $\langle S\rangle$ produced by changing the magnetic field from $H=0$ to 7 T (shown in Fig. 2) is mirrored by the accompanying *increase* in $\gamma^*(H)$. This correlation, illustrated in Fig. 13, could be understood either as a reduction in the spin degrees of freedom or as a shift in their contribution to $C_{\mathrm{mag}}(H)$, i.e., from $C_{\mathrm{anmly}}(H)$ to $\gamma^*(H)T$.

In the table in Fig. 12 the tabulated values of $S_{\mathrm{anmly}}(H)$ derived from the fit, $\langle n\rangle R\ln(2\langle S\rangle+1)$, decreased as $\langle S\rangle$ decreases from $H=0$ to 7 T. As noted in Sec. IV, it was found necessary to combine the contributions from both $\gamma^*(H)T$ and $C_{\mathrm{anmly}}(H)$ to achieve agreement between the entropies for $H=0$ and $H>0$. As expected, because of the good agreement of the fitted $C_{\mathrm{anmly}}(H)$ with the data, the combination of $\langle n\rangle R\ln(2\langle S\rangle+1)$ with $\gamma^*(H)T_0$ ($T_0=45.0$ K) gives $\langle S_{\mathrm{mag}}(H)\rangle=1.54\pm0.02\,\mathrm{J\,K^{-1}\,mol^{-1}}$ for $T=\infty$, which is in excellent agreement with $S_{\mathrm{lim}}=1.525\,\mathrm{J\,K^{-1}\,mol^{-1}}$ derived from $C(0)$.

$S_{\mathrm{lim}}=1.525\,\mathrm{J\,K^{-1}\,mol^{-1}}$ is 35% lower than that expected for the model. One might invoke an increased splitting of the crystal-field levels by the addition of ~0.14 mol O to account for the decrease in entropy, but this does not seem very probable. The reasoning given above for the change in the specific heat between $BaCuO_2$ and $BaCuO_{2.14}$ also accounts for the observed entropy reduction. As an example, the random suppression to zero of the $S=3$ spin for ~60% of the Cu_6O_{12} rings would reduce the entropy by the required amount and could also destroy long-range antiferromagnetic ordering through disruption of the superexchange linkage between clusters. (This reduction of the magnetic units by ~60% is about the same as the reduction in $\langle n\rangle$ found for the fits shown in Fig. 12.) A reduction in T_N, and the eventual suppression of antiferromagnetism, is well established as linked to an increase in the Cu valence in both $(La_{2-x}Sr_x)CuO_4$ and $YBa_2Cu_3O_{6+x}$ as x is increased.[31]

C. Other data

The measurements of specific heat reported in Ref. 10, which are the only prior measurements in magnetic fields on samples with a well-defined oxygen content, are in qualitative agreement with the present measurements. They also showed an antiferromagnetic-ordering anomaly for $BaCuO_2$

shifted to lower temperatures in magnetic fields. T_N was shifted to lower temperatures, and eventually antiferromagnetic ordering disappeared, as x increased for $BaCuO_{2+x}$. In a C/T vs T^2 plot, for low-x samples, they observed antiferromagnetic ordering, a lower-temperature Schottky-like ordering, and an upturn near 1 K—the lowest temperature of the measurements. They dismissed the possibility that this upturn near 1 K was a third ordering anomaly as observed in the present work. To account quantitatively for their specific heats for $BaCuO_{2+x}$ in the absence of a field, they invoked, as one component of the specific heat, a phenomenological, multilevel Schottky model involving large spins—they used $S=9$, although they say that other large values could also be used—and only three energy levels, each with large degeneracies. Subtraction of the specific heat for this model from the experimental data for $H\neq 0$ left a residual T-proportional term similar in magnitude to that obtained in the analysis of the present data. It was interpreted as arising from an additional lifting of the degeneracies of the three energy levels of the model that could be approximated by a continuum. For a given field, they found that $\gamma^*(H)$ *increased* with *increasing* x, which is the opposite of that reported in this paper. They also postulated an antiferromagnetic component, which was not modeled. Both components varied with x, with the antiferromagnetic component *decreasing* and the multilevel Schottky component *increasing* with *increasing* x.

They reported only one estimate of the magnetic entropy for $BaCuO_{2+x}$,1.6 $J\,K^{-1}\,mol^{-1}$, derived from the specific-heat measurements for a sample with $x=0.16$, which showed no long-range antiferromagnetic ordering. This value for the entropy is close to $S_{\rm lim}=1.525\,J\,K^{-1}\,mol^{-1}$ calculated from the specific-heat measurements for $H=0$ for $BaCuO_{2.14}$ reported in this paper.

From magnetization measurements, they deduced that $\gamma^*(H)$ is constant to $\sim$30 K and then decreases rapidly to zero at $\sim$50 K. This is consistent with the present results, which showed that $\gamma^*(H)$ had to vanish at 40–45 K to have equality between the $H=0$ and $H\neq 0$ entropies at $T=\infty$.

VII. SUMMARY

Previous magnetization, x-ray crystallographic, and neutron-diffraction measurements have shown that $BaCuO_{2+x}$ has three different Cu environments, which are independent of x, in a unit cell containing 90 formula units: There are eight Cu_6O_{12} ring clusters with an $S=3$ ferromagnetic ground state, two $Cu_{18}O_{24}$ sphere clusters with an $S=9$ ferromagnetic ground state, and six lone-spin Cu in partially occupied Cu_2O_{10} clusters.

For $BaCuO_2$ the ring clusters order antiferromagnetically with $T_N\sim 13$ K for $H=0$. T_N is shifted to a lower temperature in 7 T. The sphere clusters have short-range Schottky-like ordering in zero magnetic field, which results from a splitting of the ground state manifold for $S=9$ by a combination of crystal-electric fields and a molecular-magnetic field, which probably originates from the antiferromagnetically ordered Cu_6O_{12} ring clusters. The lone-spin Cu in the partially occupied Cu_2O_{10} clusters also have Schottky-like ordering from a splitting of the $S=1/2$ ground state by a molecular-magnetic field due to the ordered rings and/or spheres. Both Schottky-like anomalies coalesce into a single broadened one in 7 T. There is a $\gamma^*(7\ T)T$ term, not related to electronic conduction, which is presumably associated with spin degrees of freedom. The magnetic entropy derived from the specific heat is 90% of that expected for the ordering of the three structural subunits. It was necessary to include the entropy contribution from the $\gamma^*(7\ T)T$ term to achieve entropy agreement between $H=0$ and 7 T.

For $BaCuO_{2.14}$, there is no long-range antiferromagnetic ordering. The only ordering consists of short-range Schottky-like anomalies, which have a small amount of structure for low H. These anomalies can be fitted with simple Schottky functions that have a value of spin, S, which decreases as H increases. Also, as with $BaCuO_2$, there is a magnetic-field-induced $\gamma^*(H)$, which is linear in H. This increase in $\gamma^*(H)$ is correlated to the decrease in spin $\langle S\rangle$ as H is increased. The $\gamma^*(H)T$ term had to be included in $S_{\rm anmly}(H)$ to achieve entropy balance for all fields. The addition of excess oxygen, which is assumed to randomly occupy various sites in the structure, increases the Cu oxidation state. It is postulated that this oxidation state increase results in suppression of some Cu spins through covalent bonding (spin compensation) and/or formation of nonmagnetic Cu^{3+}. Vanishing of the Cu spins in some ring clusters could cause the destruction of cooperative, long-range, antiferromagnetic order through disruption of the Cu-O-Cu superexchange paths between the clusters. These superexchange paths could also be disrupted by the increase in Cu-O bond lengths as the oxygen content increases. The supposition that some Cu spins vanish is supported by the derived magnetic entropy, which is only 65% of that expected for the ordering of the three structural subunits.

ACKNOWLEDGMENTS

The work at Lawrence Berkeley National Laboratory was supported by the Director, Office of Basic Energy Sciences, Materials Sciences Division of the U.S. Department of Energy under Contract No. DE-AC03-76SF00098. Ames Laboratory is operated for the U.S. Department of Energy by Iowa State University under Contract No. W-7405-Eng-82. The work at Ames Laboratory was supported by the Director for Energy Research, Office of Basic Energy Sciences.

*Present address: Department of Chemistry and Biochemistry, Brigham Young University, Provo, Utah 84602.

†Present address: Department 530 (H/M), Samsung Information Systems America, 75 West Plumeria Drive, San Jose, California 95134.

[1] R. Kipka and H. K. Müller-Buschbaum, Z. Naturforsch. B **32**, 121 (1977); H. K. Müller-Buschbaum, Angew. Chem. Int. Ed. Engl. **16**, 674 (1977); W. Gutau and H. K. Müller-Buschbaum, J. Less-Common Met. **152**, L11 (1989).

[2] M. T. Weller and D. R. Lines, J. Solid State Chem. **82**, 21 (1989).

[3] E. F. Paulus, G. Miehe, H. Fuess, I. Yehia, and U. Löchner, J. Solid State Chem. **90**, 17 (1991); E. F. Paulus, G. Wltschek, and H. Feuss, Z. Kristallogr. **209**, 586 (1994).

[4] S. Erikson, L.-G. Johansson, L. Boerjesson, and M. Kakihana,

Physica C **162-164**, 59 (1989); T. B. Lindemer, F. A. Washburn, and C. S. MacDougall, *ibid.* **196**, 390 (1992).
[5] Z.-R. Wang, X.-L. Wang, J. A. Fernandez-Baca, D. C. Johnston, and D. Vaknin, Science **264**, 402 (1994).
[6] X.-L. Wang, J. A. Fernandez-Baca, Z.-R. Wang, D. Vaknin, and D. C. Johnston, Physica B **213-214**, 97 (1995).
[7] D. Vaknin, J. P. Koster, J. L. Zarestky, Z.-R. Wang, J. A. Fernandez-Baca, and D. C. Johnston, Phys. Rev. B **57**, 465 (1998).
[8] Z.-R. Wang, D. C. Johnston, L. L. Miller, and D. Vaknin, Phys. Rev. B **52**, 7384 (1995).
[9] X.-L. Wang, J. A. Fernandez-Baca, D. Vaknin, Z.-R. Wang, and D. C. Johnston (unpublished).
[10] J.-Y. Genoud, A. Mirmelstein, G. Triscone, A. Junod, and J. Muller, Phys. Rev. B **52**, 12 833 (1995).
[11] S. Eriksson, L-G. Johansson, L. Boerjesson, and M. Kakihana, Physica C **59**, 162 (1989).
[12] A. P. Ramirez, R. J. Cava, G. P. Espinosa, J. P. Remika, B. Batlogg, S. Zahurak, and E. A. Reitman, in *High-Temperature Superconduction*, edited by M. B. Brodsky, R. C. Dynes, K. Kitazawa, and H. L. Tuller, MRS Symposia Proceedings No. 99 (Materials Research Society, Pittsburgh, 1988), p. 459.
[13] S. J. Collocott, R. Driver, L. Dale, and S. X. Dou, Phys. Rev. B **37**, 7917 (1988).
[14] R. Kuentzler, Y. Dossmann, S. Vilminot, and S. el Hadigui, Solid State Commun. **65**, 1529 (1988).
[15] D. Eckert, A. Junod, A. Bezinge, T. Graf, and J. Muller, J. Low Temp. Phys. **73**, 24 (1988).
[16] R. Ahrens, T. Wolf, H. Wohl, H. Rietschel, H. Schmidt, and F. Steglich, Physica C **153-155**, 1008 (1988).
[17] T. Sasaki, O. Nakatsu, N. Kobayashi, A. Tokiwa, M. Kikuchi, A. Liu, K. Hiraga, Y. Syono, and Y. Muto, Physica C **156**, 395 (1988).
[18] I. Henning, M. Knobloch, and E. Hegenbarth, Phys. Status Solidi A **123**, K117 (1991).
[19] J. P. Emerson, D. A. Wright, B. F. Woodfield, J. E. Gordon, R. A. Fisher, and N. E. Phillips, Phys. Rev. Lett. **82**, 1546 (1999).
[20] D. A. Wright, J. P. Emerson, B. F. Woodfield, J. E. Gordon, R. A. Fisher, and N. E. Phillips, Phys. Rev. Lett. **82**, 1550 (1999).
[21] Z.-R. Wang, Ph.D. thesis, Iowa State University, 1994.
[22] H. J. Hoge, J. Res. Natl. Bur. Stand. **44**, 321 (1950).
[23] B. Andraka, U. Ahlheim, J. S. Kim, G. Fraunberger, G. R. Stewart, B. Morosin, E. L. Venturini, D. S. Ginley, and J. E. Schirber, Phys. Rev. B **42**, 10 016 (1990).
[24] R. A. Fisher, P. Radhakrishna, N. E. Phillips, J. V. Badding, and A. M. Stacy, Phys. Rev. B **52**, 13 519 (1995).
[25] For Nd^{3+} in Nd_2CuO_4, P. Dufour, S. Jandl, C. Thomsen, M. Cardona, B. M. Wanklyn, and C. Changlang, Phys. Rev. B **51**, 1053 (1995).
[26] For R^{3+} in $RBa_2Cu_3O_7$, H. Drössler, H.-D. Jostarndt, J. Harnischmacher, J. Kalenborn, U. Walter, A. Severing, W. Schlabitz, and E. Holland-Moritz, Z. Phys. B **100**, 1 (1996).
[27] For Nd^{3+} in $NdCu_2O_4$, R. A. Fisher, D. A. Wright, P. Radhakrishna, J. L. Luce, A. M. Stacy, and N. E. Phillips, J. Magn. Magn. Mater. **177-181**, 787 (1998).
[28] For Nd^{3+} in $Nd_{(1-x)}Sr_xMnO_4$, J. E. Gordon, R. A. Fisher, N. E. Phillips, S. F. Reklis, D. A. Wright, Y. X. Jia, and A. Zettl, J. Magn. Magn. Mater. **177-181**, 856 (1998); Phys. Rev. B **59**, 127 (1999).
[29] J. Igarashi, K. Murayama, and P. Fulde, Phys. Rev. B **52**, 15 966 (1995); P. Fulde, Physica B **230-232**, 1 (1997).
[30] W. Henggeler, B. Roessli, A. Furrer, P. Vorderwisch, and T. Chatterji, Phys. Rev. Lett. **80**, 1300 (1998).
[31] See, for example, R. A. Fisher, J. E. Gordon, and N. E. Phillips, Annu. Rev. Phys. Chem. **47**, 283 (1996).